NMR Study of the Tautomerism of Porphyrin Including the Kinetic HH/HD/DD Isotope Effects in the Liquid and the Solid State

Jürgen Braun,[1a] Martin Schlabach,[1b] Bernd Wehrle,[1c] Matthias Köcher,[1e] Emanuel Vogel,[1e] and Hans-Heinrich Limbach*,[1d]

Contribution from the Institut für Organische Chemie der Freien Universität Berlin, Takustrasse 3, D-14195 Berlin, F.R.G., and the Institut für Organische Chemie der Universität zu Köln, Greinstrasse 4, D-50939 Köln, F.R.G.

Received December 8, 1993®

Abstract: Using dynamic liquid-state ^{1}H NMR and solid-state ^{15}N CPMAS NMR spectroscopy (CP ≡ cross polarization, MAS ≡ magic angle spinning), the intramolecular double-proton transfer (tautomerism) of ^{15}N-labeled porphyrin has been studied. Rate constants including kinetic HH/HD/DD isotope effects were obtained as a function of temperature not only for the liquid phase but also for the polycrystalline solid. Within the margin of error, the liquid-state degeneracy of the tautomerism is maintained in the solid state; moreover, rate constants and kinetic isotope effects are the same for both environments. Therefore, it is justified to combine rate constants of the porphyrin tautomerism determined for various environments into a single Arrhenius diagram. The Arrhenius curves of the different isotopic reactions indicate a stepwise tautomerism via a metastable intermediate as postulated theoretically, involving thermally activated tunneling at low temperatures. Furthermore, the observed kinetic isotope effects do not support a solid-state process consisting of combined nondegenerate proton transfers and molecular 90° rotations. This possibility has been previously discussed in order to reconcile the observations of proton disorder in solid porphyrin by NMR and proton order by X-ray crystallography. Finally, a novel process has been observed which consists of a complete reversible deuteration/reprotonation of the mobile proton sites of solid porphyrin by contact with gaseous or liquid D_2O/H_2O. The process involves (i) penetration of gaseous water into the porphyrin crystals, (ii) diffusion processes of water or of porphyrin inside the crystals, and (iii) exchange of protons or deuterons in molecular hydrogen-bonded water–porphyrin complexes.

The tautomerism of porphyrins has received considerable attention.[2-35] This process consists of a double-proton transfer between the four nitrogen atoms as indicated in Figure 1. Rate constants of the thermal reaction of substituted porphyrins and hydroporphyrins dissolved in organic solvents have been obtained by different methods of dynamic NMR spectroscopy.[2-9] Full kinetic HH/HD/DD isotope effects on the tautomerism of 5,10,15,20,-tetraphenylporphyrin (TPP) were obtained some time

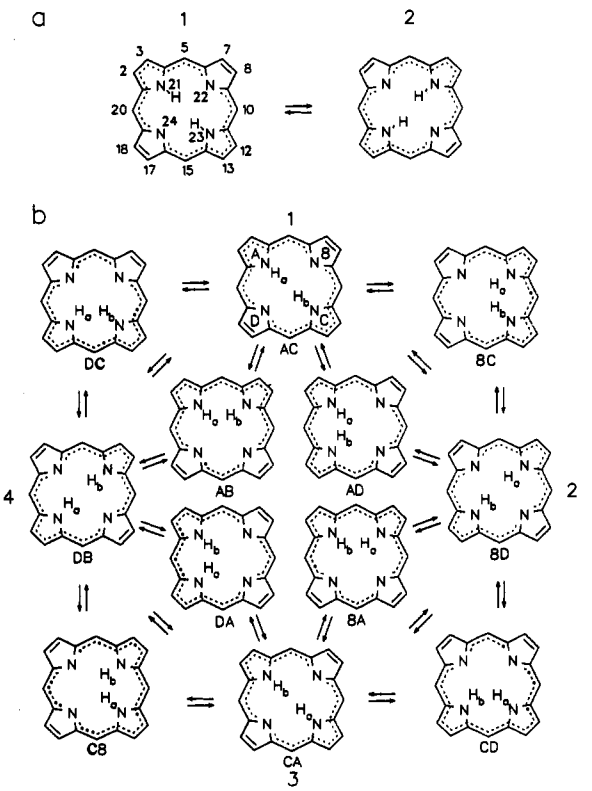

Figure 1. Degenerate tautomerism of free-base porphyrin: (a) simplified reaction model; (b) complete hydrogen-transfer pathways.

* Abstract published in *Advance ACS Abstracts*, June 15, 1994.

(1) (a) FU-Berlin. (b) Present address: Norwegian Institute for Air Research, N-2001 Lillestrøm. (c) Present address: Bayer AG, Leverkusen, Zentrale Forschung. (d) FU-Berlin; author for correspondence. (e) Universität zu Köln.

(2) Storm, C. B.; Teklu, Y. *J. Am. Chem. Soc.* **1972**, *94*, 1745. Storm, C. B.; Teklu, Y. *Ann. N. Y. Acad. Sci.* **1973**, *206*, 631.

(3) (a) Abraham, R. J.; Hawkes, G. E.; Smith, K. M. *Tetrahedron Lett.* **1974**, 1483. (b) Eaton, S. S.; Eaton, G. R. *J. Am. Chem. Soc.* **1977**, *99*, 1603. (c) Gust, D.; Roberts, J. D. *J. Am. Chem. Soc.* **1977**, *99*, 3637.

(4) (a) Yeh, H. J. C. *J. Magn. Reson.* **1977**, *28*, 365. (b) Irving, C. S.; Lapidot, A. *J. Chem. Soc., Chem. Commun.* **1977**, 184.

(5) (a) Hennig, J.; Limbach, H. H. *J. Chem. Soc., Faraday Trans. 2* **1979**, *75*, 752. (b) Hennig, J.; Limbach, H. H. *J. Am. Chem. Soc.* **1984**, *106*, 292. Hennig, J.; Limbach, H. H. *J. Magn. Reson.* **1982**, *49*, 322.

(6) Stilbs, P.; Moseley, M. E. *J. Chem. Soc., Faraday Trans. 2* **1980**, *76*, 729. Stilbs, P. *J. Magn. Reson.* **1984**, *58*, 152.

(7) Limbach, H. H.; Hennig, J.; Gerritzen, D.; Rumpel, H. *Faraday Discuss. Chem. Soc.* **1982**, *74*, 822.

(8) (a) Schlabach, M.; Rumpel, H.; Limbach, H. H. *Angew. Chem.* **1989**, *101*, 84. (b) *Angew. Chem., Int. Ed. Engl.* **1989**, *28*, 76. (c) Schlabach, M.; Scherer, G.; Limbach, H. H. *J. Am. Chem. Soc.* **1991**, *113*, 3550. (d) Schlabach, M.; Limbach, H. H.; Bunnenberg, E.; Shu, A. Y. L.; Tolf, R. R.; Djerassi, C. *J. Am. Chem. Soc.* **1993**, *115*, 4554.

(9) Schlabach, M.; Rumpel, H.; Braun, J.; Scherer, G.; Limbach, H. H. *Ber. Bunsen-Ges. Phys. Chem.* **1992**, *96*, 821.

(10) (a) Völker, S.; van der Waals, J. H. *Mol. Phys.* **1976**, *32*, 1703. (b) Völker, S.; Macfarlane, R. *IBM J. Res. Dev.* **1979**, *23*, 547. (c) Friedrich, J.; Haarer, D. *Angew. Chem.* **1984**, *96*, 96; *Angew. Chem., Int. Ed. Engl.* **1984**, *113*.

(11) Butenhoff, T.; Chuck, R. S.; Limbach, H. H.; Moore, C. B. *J. Phys. Chem.* **1990**, *94*, 7847.

(12) Webb, L. E.; Fleischer, E. B. *J. Chem. Phys.* **1965**, *43*, 3100.

(13) Fleischer, E. B.; Miller, C. K.; Webb, L. E. *J. Am. Chem. Soc.* **1964**, *86*, 2342.

(14) Chen, B. M. L.; Tulinsky, A. *J. Am. Chem. Soc.* **1972**, *94*, 4144.

(15) Tulinsky, A. *Ann. N. Y. Acad. Sci.* **1973**, *206*, 47.

(16) Hamor, M. J.; Hamor, T. A.; Hoard, J. L. *J. Am. Chem. Soc.* **1964**, *86*, 1338.

(17) Silvers, S. J.; Tulinsky, A. *J. Am. Chem. Soc.* **1967**, *89*, 3331.

0002-7863/94/1516-6593$04.50/0

ago[7] and reinvestigated recently with a higher precision.[9] Recent progress in the understanding of such effects[36-39] allowed us to interpret these effects in terms of a stepwise proton motion involving cis intermediates as shown in Figure 1b rather than in terms of a concerted transfer proposed initially.[5,7,35] The stepwise mechanism had been postulated theoretically.[31-34] Using high-resolution solid-state NMR spectroscopy[22] under the conditions of magic angle spinning (MAS), cross polarization (CP), and proton decoupling, it has been found that porphyrins and related compounds are also subject to a solid-state tautomerism.[9,23-29] Rate constants could be obtained by ^{15}N CPMAS NMR spectroscopy of the ^{15}N-labeled compounds.[9,23-26] Optical studies revealed that the parent porphyrin is also subject to a UV/Vis,[10] IR,[11] and thermally induced[30] tautomerism when embedded in Shpolski matrices at cryogenic temperatures. Rate constants, including some kinetic HH/DD isotope effects, could be obtained under these conditions. The data were compared with those obtained for TPP dissolved in liquids because of the lack of high-temperature kinetic data for the parent compound. The comparision revealed a non-Arrhenius behavior attributed to tunneling,[11,30] a phenomenon which had been proposed for a long time to play a role in the reaction.[2-9]

Since at present the theoretical treatment of the porphyrin tautomerism is restricted to the parent compound and since chemical substitution was found to increase the reaction barrier[9,24] we decided to undertake the present dynamic NMR study of the parent compound in order to establish an appropriate kinetic data basis necessary for testing different tunneling models in the future. Our objective was to measure the kinetic HH/HD/DD isotope effects not only for the liquid state but—for the first time—also for the bulk crystalline state in order to obtain information about the influence of the environment on the tautomerism. During these studies we encountered an experimental problem which has prevented us so far from determining the kinetic HH/HD/DD isotope effects on the solid-state tautomerism of porphyrins. The problem consisted in the difficulty to achieve a complete deuteration of the inner porphyrin proton sites. Moreover, it was found that during the measurements the deuterium fraction D decreased with time. A careful analysis of this phenomenon revealed that polycrystalline porphyrins can be fully deuterated by exposure either to gaseous or to liquid D_2O. Reprotonation occurs by contact with H_2O or simply with air. Exposure of the polycrystalline materials to gaseous or liquid H_2O/D_2O mixtures and sealing the samples allowed us to prepare solid porphyrins with desired time-independent deuterium fractions in the mobile proton sites and to obtain for the first time multiple kinetic HH/HD/DD isotope effects of the porphyrin tautomerism in the solid state. The results of these experiments are reported below and discussed.

The data obtained may not only be useful from a theoretical standpoint but also help to solve the problem of localizing the inner porphyrin protons by X-ray crystallography.[12-15] The problem arises because the gas-phase degeneracy of the porphyrin tautomers may be lifted in the solid state by intermolecular interactions. This phenomenon was observed by ^{15}N CPMAS NMR in the case of triclinic TPP[9,23] and other substituted porphyrins.[27-29] By contrast, the degeneracy was found to be retained in the solid state within the margin of error for *meso*-tetratolylporphyrin,[9] for a solid tetragonal solution of Ni–TPP in TPP,[23] and for the parent compound.[24] The finding of half-hydrogens on each nitrogen atom in polycrystalline porphyrin by NMR is in agreement with the X-ray structure of monoclinic porphyrin reported by Webb and Fleischer (W&F)[12] but not in agreement with the results of Chen and Tulinsky (C&T),[14,15] who found ordered protons. Since TPP forms tetragonal solid solutions with Cu–TPP[21] and with Ni–TPP,[9] exhibiting proton disorder,[21] in contrast to the case of triclinic TPP, the proton disorder in the W&F structure was ascribed to the symmetrizing effect of a hypothetical Cu–porphyrin impurity, assumed to be present to about 5–10%, in view of the observation of some electron density in the porphyrin center.[12] However, no spectroscopic evidence for this impurity was obtained. Moreover, it is a surprising but poorly discussed fact that both the W&F and the C&T structures of monoclinic porphyrin are identical with respect to the heavy atom positions in the unit cell; i.e., that they differ only with respect to the distribution of the inner protons,[12,14] in contrast to the case of TPP, where the whole crystal structure changes when metallo-TPP is present.

In order to reconcile the disagreement between NMR and the C&T structure, Frydman et al.[28,29] proposed an interesting mechanism illustrated in Figure 2a. It consists of proton-transfer steps between unequally populated tautomers, where the degeneracy observed by NMR is restored by 90° molecular rotational jumps. Evidence of the latter was obtained by ^1H and ^{13}C NMR spectroscopy.[28,29] In this report we show that the kinetic HH/HD/DD isotope effects on the tautomerism of monoclinic polycrystalline porphyrin indicate that the degeneracy of each proton-transfer step in Figure 2a is retained in the solid within the margin of error. This result does not preclude the possibility of degenerate rotations.

The paper is organized as follows. In a theoretical section the rate constants of proton and deuteron transfer and of rotation, characterizing the reaction network of Figure 2b, are related to the dynamic quantities derived by ^{15}N CPMAS NMR line-shape analysis. After an experimental section the results of all dynamic liquid- and solid-state NMR experiments are described and discussed.

(18) Codding, P. W.; Tulinsky, A. *J. Am. Chem. Soc.* **1972**, *94*, 4151.
(19) Lauher, J. W.; Ibers, J. A. *J. Am. Chem. Soc.* **1973**, *95*, 5148.
(20) Butcher, R. J.; Jameson, G. B.; Storm, C. B. *J. Am. Chem. Soc.* **1985**, *107*, 278.
(21) Schneider, M. L. *J. Chem. Soc.* **1972**, 1093.
(22) (a) Schaeffer, J.; Stejskal, E. O. *J. Am. Chem. Soc.* **1976**, *98*, 1031. (b) Fyfe, C. A. *Solid State NMR for Chemists*; C.F.C. Press: Guelph, Ontario, 1983. (c) Lyerla, J. R.; Yannoni, C. S.; Fyfe, C. A. *Acc. Chem. Res.* **1982**, *15*, 208.
(23) Limbach, H. H.; Hennig, J.; Kendrick, R. D.; Yannoni, C. S. *J. Am. Chem. Soc.* **1984**, *106*, 4059.
(24) Wehrle, B.; Limbach, H. H.; Kōcher, M.; Ermer, O.; Vogel, E. *Angew. Chem.* **1987**, *99*, 914; *Angew. Chem., Int. Ed. Engl.* **1987**, *26*, 934.
(25) Limbach, H. H.; Wehrle, B.; Schlabach, M.; Kendrick, R.; Yannoni, C. S. *J. Magn. Reson.* **1988**, *77*, 84.
(26) (a) Limbach, H. H.; Wehrle, B.; Zimmermann, H.; Kendrick, R. D.; Yannoni, C. S. *J. Am. Chem. Soc.* **1987**, *109*, 929. (b) Limbach, H. H.; Wehrle, B.; Zimmermann, H.; Kendrick, R. D.; Yannoni, C. S. *Angew. Chem.* **1987**, *99*, 241; *Angew. Chem., Int. Ed. Engl.* **1987**, *26*, 247. (c) Wehrle, B.; Zimmermann, H.; Limbach, H. H. *Ber. Bunsen-Ges. Phys. Chem.* **1987**, *91*, 941. (d) Limbach, H. H.; Wehrle, B.; Schlabach, M.; Kendrick, R.; Yannoni, C. S. *J. Magn. Reson.* **1988**, *77*, 84. (e) Wehrle, B.; Limbach, H. H.; Zimmermann, H. *J. Am. Chem. Soc.* **1988**, *110*, 7014. (f) Wehrle, B.; Limbach, H. H. *Chem. Phys.* **1989**, *136*, 223. Hoelger, Ch.; Wehrle, B.; Benedict, H.; Limbach, H. H. *J. Phys. Chem.* **1994**, *98*, 843.
(27) Frydman, L.; Olivieri, A. C.; Diaz, L. E.; Frydman, B.; Morin, F. G.; Mayne, C. L.; Grant, D. M.; Adler, A. D. *J. Am. Chem. Soc.* **1988**, *110*, 8336.
(28) Frydman, L.; Olivieri, A. C.; Diaz, L. E.; Frydman, B.; Kustanovich, I.; Vega, S. *J. Am. Chem. Soc.* **1989**, *111*, 7001.
(29) (a) Frydman, L.; Olivieri, A. C.; Diaz, L. E.; Valasinas, A.; Frydman, B. *J. Am. Chem. Soc.* **1988**, *110*, 5651. (b) Frydman, L.; Rossomando, P. C.; Sambrotta, L.; Frydman, B. *J. Phys. Chem.* **1992**, *96*, 4753.
(30) Butenhoff, T.; Moore, C. B. *J. Am. Chem. Soc.* **1988**, *110*, 8336.
(31) Kutzmitsky, V. A.; Solovyov, K. N. *J. Mol. Struct.* **1980**, *65*, 219.
(32) Sarai, A. *J. Chem. Phys.* **1982**, *76*, 5554; **1984**, *80*, 5431.
(33) Merz, K. M.; Reynolds, C. H. *J. Chem. Soc., Chem. Commun.* **1988**, 90.
(34) Smedarchina, Z.; Siebrand, W.; Zerbetto, F. *Chem. Phys.* **1989**, *136*, 285.
(35) Limbach, H. H.; Hennig, J. *J. Chem. Phys.* **1979**, *71*, 3120. Limbach, H. H.; Hennig, J.; Stulz, J. *J. Chem. Phys.* **1983**, *78*, 5432. Limbach, H. H. *J. Chem. Phys.* **1984**, *80*, 5343.
(36) Limbach, H. H. *NMR—Basic Principles and Progress*; Springer: Heidelberg, Germany, 1991; Vol. 23, Chapter 2.
(37) (a) Limbach, H. H.; Meschede, L.; Scherer, G. *Z. Naturforsch.* **1989**, *44a*, 459. Meschede, L.; Limbach, H. H. *J. Phys. Chem.* **1991**, *95*, 10267.
(38) (a) Rumpel, H.; Limbach, H. H. *J. Am. Chem. Soc.* **1989**, *111*, 5429. (b) Rumpel, H.; Limbach, H. H.; Zachmann, G. *J. Phys. Chem.* **1989**, *93*, 1812.
(39) Scherer, G.; Limbach, H. H. *J. Am. Chem. Soc.* **1989**, *111*, 5946.

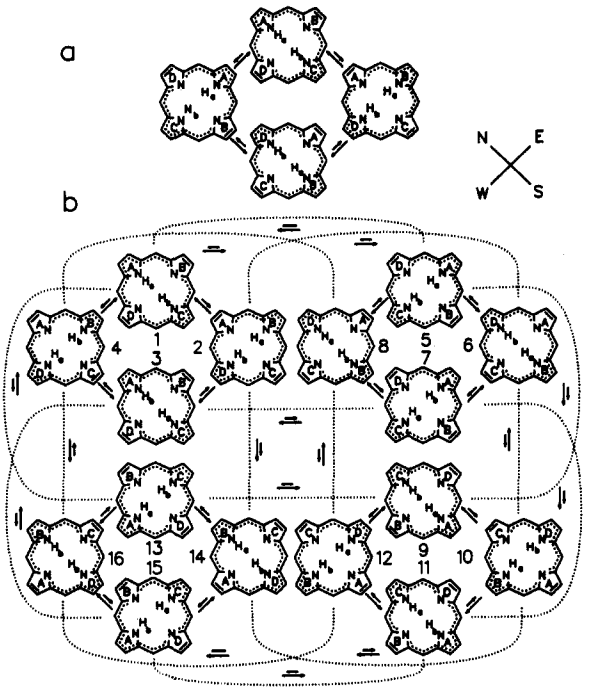

Figure 2. (a) Combined model of proton tautomerism and 90° jumps of porphyrin in the solid state according to ref 27. (b) Expanded model.

Experimental Section

Synthesis of Porphyrin-$^{15}N_4$. The synthesis of porphyrin-$^{15}N_4$ was performed as described previously,[24] in analogy to the synthesis of the nonlabeled compound which starts from pyrrole.[40] ^{15}N-labeled pyrrole was prepared from $^{15}NH_3$ and furan, in a similar way as nonlabeled pyrrole.[41] Ammonium chloride, enriched to 95% with ^{15}N, was obtained from Alfred Hempel GmbH, Düsseldorf. In order to characterize the crystallographic properties of the product used for the NMR measurements, X-ray powder spectra were taken. The cell parameters were in good agreement both with the W&F[12] and the C&T[14] structures.

Gas-Phase Deuteration and Reprotonation of Solid Porphyrin. At the beginning of this study, solid porphyrin-$^{15}N_4$-*DD* was prepared by dissolving desired amounts of the porphyrin-$^{15}N_4$-*HH* in an organic solvent mixture containing CH_3OD or C_2H_5OD and by evaporation of the solvent. The deuterium fraction *D* in the mobile proton sites was checked by ^{15}N CPMAS NMR where porphyrin-$^{15}N_4$-*HH* could easily be distinguished from porphyrin-$^{15}N_4$-*HD* and from porphyrin-$^{15}N_4$-*DD* because of the large isotope effects on the tautomerism. As mentioned in the introduction, *D* decreased slowly when the material was loaded as usual in unsealed NMR rotors, i.e. when contact with air was not strictly avoided. A closer study of this phenomenon revealed the possibility of deuterating or undeuterating polycrystalline porphyrin directly by exposure to D_2O or H_2O vapor. In order to accelerate this process, NMR sample rotors were filled with porphyrin and placed—horizontally with open ends—into an autoclave containing a separate flask of water with the desired deuterium fraction. The autoclave was then heated to 120 °C, enabling the deuteration without the solid coming into contact with liquid water. Finally, the rotor with the solid sample was removed and closed with caps and sealed with the aid of a silicon-rubber-based glue. The kinetics of the deuteration were not followed in detail, but deuteration was complete after several days, as shown by solid-state NMR. This vapor-phase deuteration was also efficiently used in the case of substituted porphyrins and related compounds. Finally, we also checked that deuteration/reprotonation of solid porphyrins also occurred when adding small amounts of liquid D_2O/H_2O to the polycrystalline solids.

Preparation of Sealed NMR Samples for Liquid-State NMR. Sealed NMR samples for liquid-state NMR were prepared using vacuum methods as decribed previously.[36] Deuteration was achieved by treatment of solid porphyrin placed in an NMR tube attached to a vacuum line filled with liquid D_2O at 120 °C for one week. During this time the D_2O was renewed twice. The liquid water was removed *in vacuo*, and any water traces were removed by condensing successively dry solvent on the sample, dissolution, and removal *in vacuo*. The degree of deuteration was later controlled by comparing the integral of the β-pyrrole proton signal with the integral of the inner proton signals.

NMR Measurements. The liquid-state NMR experiments were performed with the NMR spectrometers Bruker AMX 500 (500 MHz) and MSL 300 (300 MHz). With the latter instrument, some ^{15}N CPMAS measurements at 30.41 MHz were performed using a 5-mm high-speed spinning probehead from Doty Scientific (Columbia SC). However, most of the spectra were measured with a Bruker CXP 100 NMR spectrometer equipped with a 2.1-T wide-bore cryomagnet (90 MHz for ^{1}H, 9.12 MHz for ^{15}N) and a standard 7-mm Doty CPMAS NMR probehead. In the low-temperature experiments, the driving nitrogen gas was cooled with liquid nitrogen using a home-built heat exchanger as described previously.[42] In order to remove rotational side bands which complicate the line-shape analysis, spinning speeds of 2–3 and 8–9 kHz were employed at 2.1 and 7 T, respectively. Since high-speed spinning leads to sample heating,[43] a small amount of the ^{15}N chemical shift thermometer TTAA[43] was added to the sample which contributes four sharp lines to the spectra with temperature-dependent line positions. The sample temperatures were obtained from the latter as described previously.[43] All spectra were obtained with a pulse sequence used for solid-state T_1 experiments[44] and a mixing time of 1 s. The result of this sequence is that the line intensities of protonated and nonprotonated nitrogen atoms are no longer distorted by different cross polarization times, an effect arising from spectral spin diffusion among abundant ^{15}N spins.[25]

Theoretical Section

The methods for obtaining rate constants of the tautomerism of porphyrins by liquid-state ^{1}H NMR and solid-state ^{15}N CPMAS NMR spectroscopy have recently been reviewed in detail[8,9,36] and need not be repeated here. However, the influence of—detectable only in the solid state—rotational 90° jumps of porphyrin molecules and their deuterated analogs in a crystalline environment on the ^{15}N CPMAS NMR spectra according to Figure 2 has not yet been evaluated. The appropriate line-shape equations are set up in the appendix. Here, we discuss the conditions under which the rotational 90° jumps will show up in the ^{15}N CPMAS NMR spectra. We will only consider modulations of isotropic chemical shifts by the various processes and neglect possible effects arising from a modulation of anisotropic chemical shifts and of dipolar interactions.

Effect of Molecular Rotations of Porphyrin on Its ^{15}N CPMAS NMR Spectra. Each reaction step in Figure 2a consists either of a proton transfer or a rotational 90° in-plane jump, which implies the possibility of several consecutive proton transfers or several consecutive 90° jumps. As this circumstance is not well expressed by Figure 2a, we take, therefore, the complete network illustrated in Figure 2b into consideration, where the different molecular states in Figure 2b are labeled sequentially. Rate constants relating states *i* and *j* are then labeled as $k_{i,j}$. The states with inner protons north and south are assumed to be favored over the states with protons east and west. The rotation is characterized by the forward and backward rotational rate constants

$$k_{1,5} = k_{1,13}, \ldots, k_{5,1} = k_{13,1}, \ldots \quad (1)$$

In the liquid state the "horizontal" proton transfers, e.g. 1 → 2, and the "vertical" proton transfers, e.g. 1 → 4, are equivalent. This equivalence may be lifted in the solid state. In this case it

(40) Longo, F. R.; Thorne, E. J.; Adler, A. D.; Dym, S. *J. Heterocycl. Chem.* **1975**, *12*, 1305.
(41) Ryskiewicz, E. E.; Chaikin, S. W. *J. Am. Chem. Soc.* **1954**, *76*, 4485.
(42) Kendrick, R. D.; Friedrich, S.; Wehrle, B.; Limbach, H. H.; Yannoni, C. S. *J. Magn. Reson.* **1985**, *65*, 159.
(43) Wehrle, B.; Aguilar-Parrilla, F.; Limbach, H. H. *J. Magn. Reson.* **1990**, *87*, 584. Wehrle, B.; Aguilar-Parrilla, F.; Limbach, H. H. *J. Magn. Reson.* **1990**, *87*, 592.
(44) Torchia, D. *J. Magn. Reson.* **1978**, *30*, 1978.
(45) Kubo, R. *Nuovo Cimento Suppl.* **1957**, *6*, 1063. Sack, R. A. *Mol. Phys.* **1958**, *1*, 163. Binsh, G. *J. Am. Chem. Soc.* **1969**, *91*, 1304.

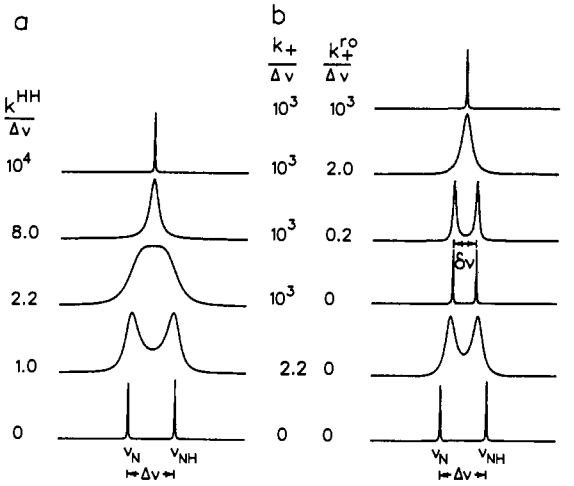

Figure 3. Calculated ^{15}N CPMAS NMR spectra of combined proton transfer in porphyrin and rotation of the whole molecule in porphyrin in the case of (a) $K = 1$ and (b) $K < 1$. For further explanations see text.

follows from Figure 2b that

$$k_{1,2} = k_{6,7} = \ldots \neq k_{1,4} = k_{8,7} = \ldots \quad (2)$$

The equilibrium constants of tautomerism and of rotation are equal, i.e.

$$K = k_{1,5}/k_{5,1} = k_{1,2}/k_{2,1} = k_{1,4}/k_{4,1} \quad (3)$$

Note, however, that the kinetics of both processes may be different; i.e., *a priori*, rotation could be either slower or faster than proton transfer.

The ^{15}N NMR line-shape theory of this problem is easily set up according to well-known rules.[44] As described in the appendix, a set of coupled differential equations of dimension 16 results for the network of Figure 2b which reduces to dimension 4 in the porphyrin case where the chemical shifts of all protonated nitrogen atoms are given by the same value ν_{NH} and those of the nonprotonated atoms by ν_N. The rate constants obtained by line-shape analysis are given by

$$k_+ = k_{1,2} + k_{1,4} = \ldots, k_+^{ro} = k_{1,5} + k_{1,13} = \ldots = 2k_{1,5} = 2k_{1,13} \ldots \quad (4)$$

$$k_- = k_{2,1} = k_{4,1} = \ldots, k_-^{ro} = k_{5,1} + k_{13,1} = \ldots = 2k_{5,1} = 2k_{13,1} \ldots \quad (5)$$

where k_+ and k_- are the overall rate constants of the forward and the backward proton transfer and k_+^{ro} and k_-^{ro} those of the rotation. In the following, we discuss some special cases important in the context of the porphyrin tautomerism.

A. Truly Symmetrical Case with K = 1. Here, the ^{15}N CPMAS NMR line shapes become independent of the rate constants $k_+^{ro} = k_-^{ro} = k^{ro}$ of rotation. The parameter extracted by line-shape analysis is given by

$$k = k_+ = k_{1,2} + k_{1,4} = k_- = k_{2,1} + k_{4,1} \quad (6)$$

The usual line-shape changes are expected, as illustrated in Figure 3a. At low temperatures two lines appear for the protonated and the nonprotonated nitrogen atoms characterized by the chemical shifts ν_{NH} and ν_N. The lines broaden and coalesce into a single sharp center line as k is increased.

B. Unsymmetrical Case with K < 1 Where Proton Tautomerism Is Faster than Rotation. In this case the two lines broaden, move toward each other, and sharpen again without coalescence as shown in Figure 3b, when the rate of proton transfer k_+ is increased. In the fast-proton-transfer regime, the splitting between the lines is given by[22,25]

$$\delta\nu = \Delta\nu(1 - K)/(1 + K), \Delta\nu = \nu_N - \nu_{NH} \quad (7)$$

Now, an increase of the rates of rotation k_+^{ro} leads to line broadening and coalescence into a single center line as shown in Figure 3b. In this regime a rate constant k^{ro} of an apparently symmetric two-state problem can be defined and related to the rates of rotation by

$$k^{ro} = 2k_+^{ro}/(1 + K) \quad (8)$$

C. Unsymmetrical Case with K ≪ 1. The east–west tautomers now have such a high energy that they are no longer directly observable. As shown in the appendix a symmetrical two-state problem results. If the rotation is fast and proton transfer slow, the observable rate constant is given by

$$k = 2k_+ = 2(k_{1,2} + k_{1,4}) \text{ for } k_{5,1} \gg k_{2,1}, k_{4,1} \quad (9)$$

If the rotation is fast and the proton transfer slow, it follows that

$$k^{ro} = 4k_{1,5} \text{ for } k_{5,1} \ll k_{2,1}, k_{4,1} \quad (10)$$

The validity of eqs 6–10 was controlled by numerical line-shape simulations.

Kinetic HH/HD/DD Isotope Effects. The previous treatment refers to the transfer of two protons. The equations derived are also valid for the transfer of two deuterons. However, the case where one proton and one deuteron migrate requires further comment. This case is included in Figures 1 and 2 by setting H_a = H and H_b = D. The inverse definition H_a = D and H_b = H is equivalent in the absence of equilibrium isotope effects, an assumption which is well fulfilled in the case of porphyrins within the margin of error of NMR spectroscopy. The isotope effects depend on the pathway of the proton motion. Because of all experimental and theoretical evidence in favor of a stepwise motion in porphyrins, in the following the case of a concerted motion is not taken into consideration.

A. Symmetrical Case with K = 1. From eq 6 it follows that the rates of rotation do not influence the observed rates of proton transfer, and we need only discuss the isotope effects on the proton-transfer steps of Figure 1b. The observed rate constants defined in eq 6 have then to be labeled as k^{LL}, where LL = HH, HD, DD. Theoretical expressions for the kinetic isotope effects on the degenerate stepwise double-proton transfer in porphyrins have been derived previously[7-9] and can be written using eq 6 in the form

$$k^{HH}/k^{DD} = PS, k^{HD}/k^{DD} = 2/(P^{-1} + S^{-1}), k^{LL} = k_{1,2}^{LL} + k_{1,4}^{LL}, \text{LL} = \text{HH, HD, DD} \quad (11)$$

P represents the primary isotope effect arising from the mobile proton in flight, and S, the secondary isotope effect arising from the bound mobile proton. Since $S \approx 1$ and $P \gg 1$, it follows that

$$k^{HH}/k^{DD} \approx P, k^{HD}/k^{DD} \approx 2 \text{ for } P \gg 1 \quad (12)$$

This result is visualized in Figure 4a, where the free energy reaction pathways for the selected pathway 5 → 1 → 2 → 6 from Figure 2b are depicted for the various isotopic reactions. Rotational jumps between 5 and 1 and between 2 and 6 are assumed to be fast. In the HH and DD cases, the reaction profile does not depend on which particle a or b is transferred first. In the HD case the transfer of D is rate-limiting and occurs either in the first or the second step. This barrier has the same height as those of the DD reaction. Nevertheless, the HD reaction is faster than the DD reaction by a factor of 2 (eq 12) because there is only

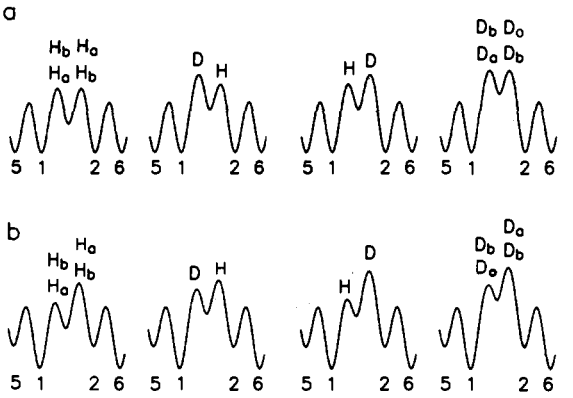

Figure 4. Free energy reaction profiles (schematically) of the stepwise HH, DH, HD, and DD tautomerism of porphyrin combined with molecular 90° rotations in the solid state based on the reaction network of Figure 2. For simplicity, only a reduced number of states is shown. Reactions 5 → 1 and 2 → 6 refer to a 90° rotation, and reaction 1 → 2 refers to the tautomerism: (a) symmetrical case with $K = 1$; (b) asymmetrical case with $K \ll 1$.

one rate-limiting barrier in the HD case but two equal barriers in the DD case. Equation 12 was found to be valid in a number of symmetric porphyrins.[7-9]

B. Unsymmetrical Case with K ≪ 1. In the cases where hydrogen transfer is much faster than rotation, no isotope effects are expected, and this case can easily be verified experimentally. Therefore, we only continue to discuss the case where rotation is much faster than hydrogen transfer, leading to a reaction profile as illustrated schematically in Figure 4b. The kinetic isotope effects of the tautomerism of unsymmetrical porphyrins have recently been evaluated.[7-9] In the limit where the asymmetry is large, the problem simplifies and the situation can be rationalized as follows.

A look at Figure 1b indicates that in the case where the tautomers 2 = DB and 4 = BD exhibit a higher energy than the tautomers 1 = AC and 3 = CA—caused by intermolecular interactions in the solid state—the intermediates BC, AD, AB, and DC are also no longer equivalent. Assuming that the energy of AD is larger than that of BC, only the process AC → BC → BD is relevant, where H_a is transferred before H_b, and the process AC → AD → BD, where H_b is transferred first, no longer contributes to the rate of interconversion between 1 and 2. The corresponding reaction profiles are illustrated in Figure 4b. By inspection, it follows that

$$k_{1,2}^{DH} \approx k_{1,2}^{HH} \text{ and } k_{1,2}^{HD} \approx k_{1,2}^{DD} \quad (13)$$

because in the DH process an H is transferred in the rate-limiting step and in the HD process a D is transferred. Similar relations also hold for proton transfer between states 1 and 4. As indicated in eq 9, the quantities

$$k^{HH} = 2(k_{1,2}^{HH} + k_{1,4}^{HH}),\ k^{DD} = 2(k_{1,2}^{DD} + k_{1,4}^{DD}),\ k^{HD} = (k_{1,2}^{HD} + k_{1,4}^{HD} + k_{1,2}^{DH} + k_{1,4}^{DH}) \quad (14)$$

are obtained experimentally. Using eq 13, it then follows that

$$k^{HD} \approx (k_{1,2}^{DD} + k_{1,4}^{HH} + k_{1,2}^{HH} + k_{1,4}^{DD}) \quad (15)$$

By combination of eqs 13 and 14, we obtain

$$k^{HH}/k^{DD} = (k_{1,2}^{HH} + k_{1,4}^{HH})/(k_{1,2}^{DD} + k_{1,4}^{DD}),\ k^{HD}/k^{DD} = (k_{1,2}^{DD} + k_{1,4}^{HH} + k_{1,2}^{HH} + k_{1,4}^{DD})/(k_{1,2}^{DD} + k_{1,4}^{DD}) \quad (16)$$

Assuming similar primary isotope effects P for the 1 → 2 and the 1 → 4 processes, it follows that

$$k^{HH}/k^{DD} = (Pk_{1,2}^{DD} + Pk_{1,4}^{DD})/(k_{1,2}^{DD} + k_{1,4}^{DD}),\ k^{HD}/k^{DD} = (k_{1,2}^{DD} + Pk_{1,4}^{DD} + Pk_{1,2}^{DD} + k_{1,4}^{DD})/(2k_{1,2}^{DD} + 2k_{1,4}^{DD}) \quad (17)$$

i.e.

$$k^{HH}/k^{DD} = P,\ k^{HD}/k^{DD} = (P+1)/2,\ k^{HH}/k^{HD} \approx 2P/(P+1) \quad (18)$$

By comparison with eq 11, it follows that the cases $K = 1$ and $K \ll 1$ can be distinguished by measuring the kinetic HH/HD/DD isotope effects on the tautomerism of porphyrin in the solid state. If $K = 1$, the HD reaction is approximately twice as fast as the DD reaction (eq 12). If $K \ll 1$, the rate constants of the HD reaction are half of those of the HH reaction (eq 18). Note that eqs 14–18 were derived in a more rigorous way in ref 8c; in addition, eq 18 was verified experimentally in the case of *meso*-tetraphenylchlorin, where the symmetry of the tautomerism is perturbed by chemical modification.[8c]

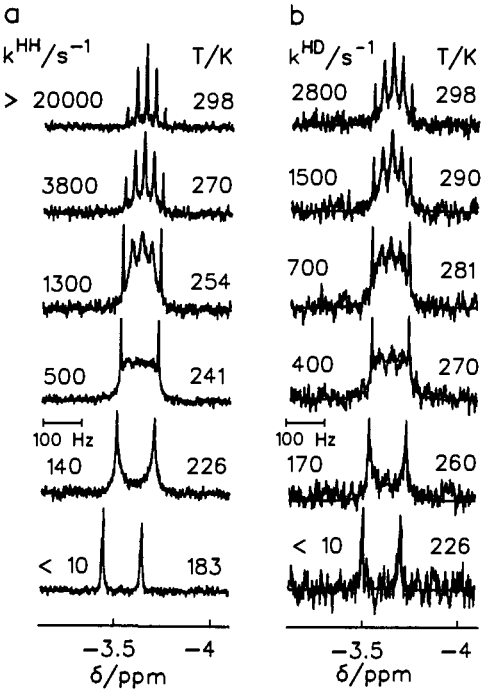

Figure 5. Superposed experimental and calculated 500-MHz ^{1}H NMR spectra of the inner protons of porphyrin-$^{15}N_4$ dissolved in toluene-d_8 (~1 mmol L^{-1}): (a) deuterium fraction $D = 0$ of the inner proton sites; (b) $D = 0.9$. 6.5-μs pulse length with π/2 pulses of 10 μs, 9-kHz spectral width, 3.5-s repetition time.

Results

Kinetic HH/HD/DD Isotope Effects on the Tautomerism of Porphyrin-$^{15}N_4$ Dissolved in Toluene-d_8. In this section, we describe the dynamic ^{1}H NMR experiments performed on porphyrin-$^{15}N_4$ dissolved in toluene-d_8 at different deuterium fractions D in the mobile proton sites. The superposed experimental and calculated 500-MHz ^{1}H NMR signals of the inner porphyrin protons are shown in Figure 5 as a function of temperature at $D = 0$ and 0.9. In both cases the tautomerism gives rise to a doublet–pentet transition of the inner proton signal as temperature is increased, a phenomenon which has been described frequently for symetrically substituted ^{15}N-labeled porphyrins.[4,5,8,9] The rate constants were obtained as usual by line-shape analysis. The values of the coupling constant $J_{^1H-^{15}N}$ and the residual line width in the absence of exchange, W_0, were

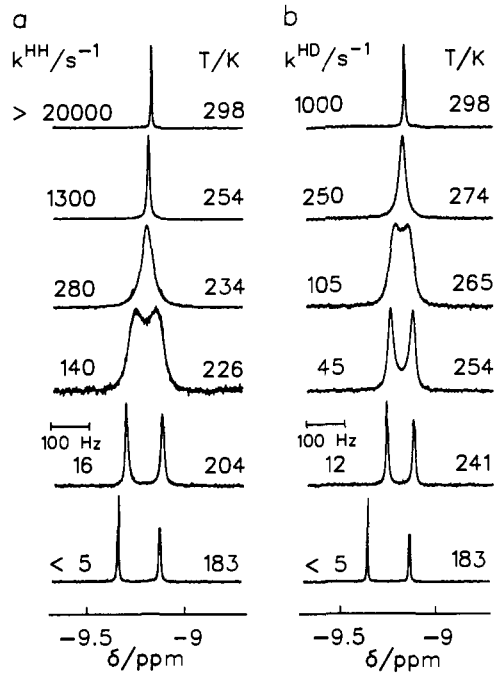

Figure 6. Superposed experimental and calculated 500-MHz ^{1}H NMR spectra of the β-pyrrole protons of porphyrin-$^{15}N_4$ dissolved in toluene-d_8 (~1 mmol L^{-1}): (a) $D = 0$; (b) $D = 0.99$. Same conditions as in Figure 5.

obtained by simulation of the outer line components. At low temperature the doublet is asymmetric; i.e., the two lines exhibit differential transverse relaxation times. This phenomenon arises from an increase in the rotational molecular correlation times and an interference between relaxation via dipolar interactions and the chemical shift anisotropy.[46] At a deuterium fraction of $D = 0$ in the inner proton sites, the signal only stems from porphyrin-*HH*; the line shape, therefore, depends only on the rate constants $k^{HH} = k^{HH}_{1,2} + k^{HH}_{1,4} = 2k^{HH}_{1,2} = 2k^{HH}_{1,4}$ (see Figure 1). At $D = 0.9$ the signal stems to 90% from porphyrin-*HD* and to 10% from porphyrin-*HH*; i.e., the line shapes depend dominantly on the rate constants $k^{HD} = k^{HD}_{1,2} + k^{HD}_{1,4} = 2k^{HD}_{1,2} = 2k^{HD}_{1,4}$ and to a minor extent on k^{HH}. In the simulation, the presence of porphyrin-*HH* was taken into account. In view of the low solubility of porphyrin in organic solvents, it is clear that the signal-to-noise ratio at $D = 0.9$ (Figure 5b) is much poorer than that at $D = 0$ (Figure 5a).

Parts a and b of Figure 6 show the superposed experimental and calculated 500-MHz ^{1}H NMR signals of the β-pyrrole signals of porphyrin dissolved in toluene-d_8, at $D = 0$ and 0.99. In the slow-proton-exchange regime, two signals are observed at 9.08 and 9.30 ppm assigned previously to the nonprotonated and the protonated pyrrole rings.[2,29] These values are slightly different from those found when using CD_2Cl_2 as solvent.[29] For the ^{15}N-labeled porphyrin, a small doublet splitting of 3.2 Hz arising from scalar coupling between the β-pyrrole protons of the nonprotonated rings and the corresponding ^{15}N atoms is observed. The corresponding coupling in the protonated pyrrole rings is too small to be noticeable. As temperature is increased, the lines broaden, coalesce, and sharpen again into a doublet characterized by a splitting of 1.6 Hz. This value represents the average of the β-pyrrole proton ^{15}N coupling of the two types of rings. The simulations of the spectra in Figure 6 are straightforward. Below 265 K, the chemical shift values required for the simulations in Figure 6a were taken from the spectra of Figure 6b because no isotope effects on the chemcial shift were observed. Since the values of k^{HH} were already known from the simulation of the inner proton signals, only the line width W_0 in the absence of exchange needed to be adapted. These values were then used in the simulation of the spectra in Figure 6b, thus allowing the determination of k^{DD} below 265 K without assumptions. Above 265 K, chemical shift values extrapolated from low temperature were used to calculate the spectra in Figure 6b. The kinetic HH/DD isotope effects are clearly demonstrated by comparison of the two sets of spectra.

All data obtained by line-shape simulation are assembled in Table 1. A linear least squares fitting of the data leads to the following expressions for the tautomerism of porphyrin dissolved in toluene-d_8:

$$k^{HH} = 2k^{HH}_{AC\rightarrow DB} = 10^{10.7}\exp(-37.1\ \text{kJ mol}^{-1}/RT),\quad 209\ \text{K} \le T \le 309\ K,\ 2k^{HH}_{AC\rightarrow DB}(298) \approx 16\,000\ \text{s}^{-1} \quad (19)$$

$$k^{HD} = 2k^{HD}_{AC\rightarrow DB} = 10^{11.2}\exp(-44.8\ \text{kJ mol}^{-1}/RT),\quad 260\ \text{K} \le T \le 311\ \text{K},\ 2k^{HD}_{AC\rightarrow DB}(298) \approx 2360\ \text{s}^{-1} \quad (20)$$

$$k^{DD} = 2k^{DD}_{AC\rightarrow DB} = 10^{11.4}\exp(-47.3\ \text{kJ mol}^{-1}/RT),\quad 240\ \text{K} \le T \le 298\ \text{K},\ 2k^{DD}_{AC\rightarrow DB}(298) \approx 1190\ \text{s}^{-1} \quad (21)$$

From these equations we obtain the following kinetic isotope effects at 273 K

$$k^{HH}/k^{DD} \approx 17,\ k^{HD}/k^{DD} \approx 1.9 \quad (22)$$

Solid State ^{15}N CPMAS NMR Studies of Porphyrin-$^{15}N_4$. Figure 7 depicts the superposed experimental and calculated ^{15}N CPMAS NMR spectra of ^{15}N-labeled porphyrin as a function of temperature at 2.1 and 7 T, corresponding to 9.12 and 30.41 MHz. The signals of the added ^{15}N chemical shift thermometer TTAA[42] used to calculate the sample temperatures are indicated by asterisks in Figure 7b.

The spectral changes observed reproduce those described previously.[24] At low temperatures, a high-field line is observed at 109 ppm for the protonated nitrogen atoms and a low field line at 218 ppm for the nonprotonated nitrogen atoms. As temperature is increased the lines broaden due to the proton transfer and coalesce into a single line. The spectra at 7 T were measured in order to detect possible line-shape features arising from a slow molecular rotation as illustrated in Figure 3b, but such features could not be detected. In other words, it was possible to simulate—within the margin of error—all spectra of Figure 7 in terms of the simple symmetric two-state model characterized by a single rate constant k and an equilibrium constant of tautomerism $K = 1$. In the slow-exchange regime the high-field is slightly broader than the low-field line.[24] The width of this line—measured in Hz—increases with the strength of the magnetic field but remains constant in the ppm scale. This result indicates that the high-field line consists of two nonresolved lines with slightly different chemical shifts. In other words, there seems to be a slight deviation from D_{2h} symmetry at low temperatures which, however, does not significantly perturb the degeneracy of the tautomerism.

In order to obtain the kinetic HH/HD/DD isotope effects on the solid-state tautomerism of porphyrin, a set of experiments was performed at 2.1 T as a function of temperature and the deuterium fraction D in the mobile proton sites. In a first stage, spectra were obtained at $D = 0$, some of which are shown in Figures 7a and 8a. The sample was then exposed to D_2O vapor for several days, as described in the Experimental Section. In order to achieve the highest deuterium fraction possible, D_2O was renewed twice. Several of the resulting spectra from which the rate constants k^{DD} were obtained by simulation are shown in

(46) See for example: Shimidzu, H. *J. Chem. Phys.* **1964**, *40*, 3357. Rûterjans, H.; Kaun, E.; Hull, W. E.; Limbach, H.-H. *Nucleic Acids Res.* **1982**, *10*, 7027. Gueron, M.; Leroy, J. L.; Griffey, R. H. *J. Am. Chem. Soc.* **1983**, *105*, 7262.

Table 1. Results of the ^1H NMR Experiments on Porphyrin Dissolved in Toluene-d_8[a]

T/K	method	k^{HH}/s^{-1}	k^{HD}/s^{-1}	k^{DD}/s^{-1}	D	$\Delta\nu$/Hz	W_0/Hz	W_0/Hz[g]
209	NH	32			0	99.2	3.6	
220	NH	81			0	99.2	3.5	
226	NH	145			0	97.5		3.0, 3.5
229	NH	144			0	96.0	3.0	
232	NH	200			0	97.9	3.5	
234	NH	280			0	97.0		3.0, 3.5
241	NH	480			0	97.7	3.0	
241	NH	500			0	97.0		3.0, 3.5
242	NH	500			0	97.5	3.0	
248	NH	670			0	97.0	3.0	
254	NH	1130			0	97.4	3.0	
254	NH	1300			0	97.0		3.0, 3.3
260	NH	1800			0	97.7	4.1	
260	NH	1800			0	97.0		3.0, 3.2
270	NH	3800			0	97.0		3.0, 3.0
273	NH	4400			0	97.0	2.3	
275	NH	4440			0	97.5	2.8	
289	NH	11 000			0	97.0	2.0	
299	NH	18 000			0	97.0	2.1	
301	NH	17 000			0	97.5	2.5	
309	NH	32 000			0	97.0	2.5	
209	Py	37			0	55[c]	0.9	
220	Py	82			0	51[c]	3.2	
226	Py	145			0	81[e]	2.0	
232	Py	190			0	45[e]	1.4	
234	Py	280			0	69[e]	2.0	
241	Py	500			0	64[e]	2.0	
254	Py	1300			0	62[e]	2.0	
260	Py	1800			0	58[e]	2.0	
270	Py	3800			0	53[e]	2.0	
260	NH	1735[b]	140		0.9	98.5	6.5	
260	NH	1735[b]	170		0.9	97.0		3.5, 3.7
263	NH	2110[b]	260		0.9	98.5	6.5	
270	NH	3280[b]	400		0.9	97.0		3.5, 3.5
273	NH	3935[b]	520		0.9	97.5	4.5	
281	NH	6275[b]	700		0.9	97.0		3.5, 3.5
284	NH	7420[b]	860		0.9	97.5	7.5	
290	NH	10 280[b]	1500		0.9	97.0		3.5, 3.5
295	NH	13 350[b]	1800		0.9	97.5	5.5	
298	NH	15 550[b]	2800		0.9	97.0		3.5, 3.5
214	Py	43[b]	2[b]		0.9	54[c]	1.6	
230	Py	185[b]	10[b]		0.9	46[c]	1.7	
240	Py	415[b]	28[b]	12	0.9	43[d]	1.5	
250	Py	870[b]	68[b]	25	0.9	40[d]	3.3	
260	Py	1735[b]	155[b]	75	0.9	37[d]	6.0	
274	Py	4180[b]	448[b]	240	0.9	35[d]	1.5	
289	Py	9745[b]	1250[b]	700	0.9	34[d]	1.0	
254	Py			45	1.0	62[e]	2.3	
256	Py			60	1.0	59[e]	2.3	
260	Py			77	1.0	58[e]	2.3	
265	Py			105	1.0	57[e]	2.3	
270	Py			210	1.0	53[f]	2.3	
274	Py			250	1.0	50[f]	2.3	
298	Py			1000	1.0	33[f]	2.3	

[a] Solvent: Tol = toluene-d_8, THF = tetrahydrofuran-d_8. Method: NH, ^1H NMR line-shape analysis of the ^1H–^{15}N signals ($\Delta\nu = {}^1J_{H-^{15}N}$); Py, ^1H NMR line-shape analysis of the β-pyrrole signals ($\Delta\nu$ = difference of chemical shifts). $k^{LL} = 2k^{LL}_{AC\rightarrow DB}$, LL = HH, HD, and DD. D: deuterium fraction determined by line-shape analysis at a temperature where the rate constant $k^{HH} \gg \Delta\nu$ whereas k^{HD}, $k^{DD} \ll \Delta\nu$. W_0: line width in the absence of exchange, determined by comparison with signals which do not show exchange broadening. [b] Calculated according to eqs 19 and 20. [c] Determined by line-shape analysis of the β-pyrrole signals at $D = 0.9$ at the same temperature. [d] Determined by line-shape analysis from the spectra observed at 500 MHz with $D = 1$. [f] Determined by extrapolation from *e*. [g] Different line width for the *N* and NH line due to CSA relaxation; for more explanations see text.

Figure 8c. Contributions arising from the HH- and the HD-species were neglected in these simulations. Deuteration raises the coalescence point to about 30 K, revealing large kinetic HH/DD isotope effects on the solid-state tautomerism. No change of the deuterium fraction as a function of time was observed, indicating that the rotor caps were efficiently sealed to the rotor.

In the last stage, the sample was exposed to water vapor containing a deuterium fraction of $D = 0.2$, which, in the statistical limit, should lead to the isotopic porphyrin mole fractions of $x_{HH} = (1 - D)^2 = 0.64$, $x_{HD} = 2(1 - D)D = 0.34$, and $x_{DD} = D^2 = 0.04$. The resulting spectra are shown in Figure 8b. Because of the use of the ^1H–^{15}N cross polarization technique, the apparent populations of the different isotopic species, p_{HH}, p_{HD}, and p_{DD} are not equal to the real mole fractions. Shorter CP times decrease the contribution of porphyrin-*DD*. Therefore, in the simulation of the spectra in Figure 7b, p_{DD} was neglected. Intensity distortions between the two nitrogen signals of a given isotopic species, caused by both the tautomerism and spin diffusion,[25] were removed by magnetization transfer prior to detection, as described in the Experimental Section. In other words, the spectra in Figure 8b could be simulated in terms of a superposition of two symmetric two-state exchange systems, one for porphyrin-*HH* and one for porphyrin-*HD*. Only one population parameter, $p_{HD} = 1 - p_{HH}$, and one rate constant, k^{HD}, needed to be adapted, because the values of k^{HH} were already known from the

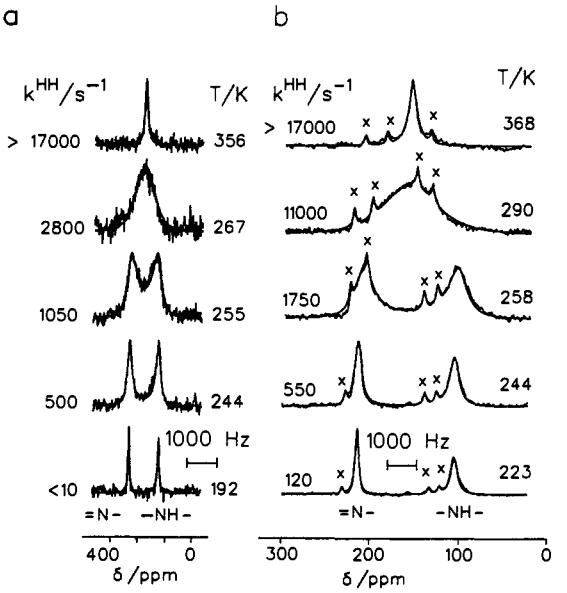

Figure 7. Superposed experimental and calculated ^{15}N CPMAS NMR spectra of porphyrin-$^{15}N_4$ as a function of temperature: (a) ^{15}N CPMAS NMR at 9.12 MHz, 3–7-ms CP time, 7-kHz spectra width, 3.1-s repetition time, 2–3-kHz spinning speed; (b) ^{15}N CPMAS NMR at 30.41 MHz, 3–9-ms CP time, 22-kHz spectra width, 3.6-s repetition time, 8–9-kHz spinning speed.

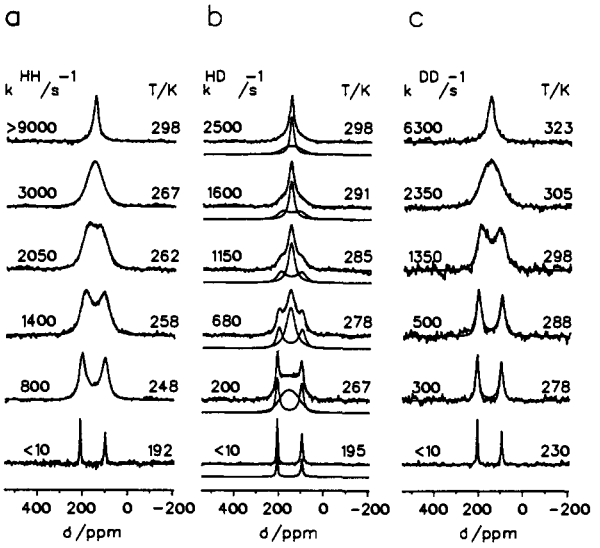

Figure 8. Superposed experimental and calculated ^{15}N CPMAS NMR spectra of porphyrin-$^{15}N_4$ at 9.12 MHz as a function of temperature and deuterium fraction D in the mobile proton sites. Experimental conditions: 3–7-ms CP time, 7-kHz spectra width, 3.3-s repetition time, 2–3-kHz spinning speed, (a) $D = 0$, (b) $D = 0.2$, (c) $D > 0.95$.

Table 2. Rate Constants of the Tautomerism of Solid Porphyrin

T/K	k^{HH}/s^{-1}	k^{HD}/s^{-1}	k^{DD}/s^{-1}	p_{HD}	method[a]
223	120				3
244	500				1
244	550				3
248	800				2
253	1000				2
255	1050				1
258	1400				2
258	1750				3
261	1700				1
262	2050				2
263	1950				1
267	2800				1
267	3000				2
267		300		0.58	2
274		550		0.56	2
278		680		0.56	2
281		900		0.56	2
285		1150		0.56	2
290	11 000				3
291		1600		0.56	2
293			1100		2
298		2500	1350	0.56	2
305			2350		2
306		4200		0.56	2
310			2600		2
320			6300		2
368	17 000				3

[a] Method 1: ^{15}N CPMAS NMR at 9.12 MHz, $\Delta\nu$ = 980 Hz, W_0(NH) = 68 Hz, W_0(N) = 57 Hz, 2.0–3.0-kHz spinning speed. Method 2: ^{15}N CPMAS NMR at 9.12 MHz, $\Delta\nu$ = 980 Hz, W_0(NH) = 80 Hz, W_0(N) = 55 Hz, 2.5–2.9-kHz spinning speed, p_{HD} = population of the HD species with $p_{HH} + p_{HD} = 1$; for further explanation see text. Method 3: ^{15}N CPMAS NMR at 30.41 MHz, $\Delta\nu$ = 3305 Hz, W_0(NH) = 215 Hz, W_0(N) = 120 Hz, 8.0–9.0-Hz spinning speed.

experiments at $D = 0$. p_{HD} depended slightly on temperature because of the temperature-dependent CP dynamics and was found to vary between 0.58 and 0.56. For the sake of clarity, the individual theoretical line shapes of porphyrin-*HH* and porphyrin-*HD* are included in Figure 8b. It is obvious that good rate constants k^{HD} could be obtained because both line-shape contributions can be well separated. From a comparison of the line-shape contributions of the HD-species with the lines in Figure 8c at comparable temperatures, it follows immediately that k^{HD} is somewhat larger than k^{DD}. This corroborates the assumption that the contributions of the HH- and the HD-species in the line-shape analysis of Figure 8c can be neglected. The deuteration and reprotonation experiments on porphyrin were repeated several times, and each time identical values of k^{HH}, k^{HD}, and k^{DD} were found.

All parameters used in the line-shape calculations are listed in Table 2. We obtain the following Arrhenius equations:

$$k^{HH} = 2k^{HH}_{AC\rightarrow DB} = 10^{11.1}\exp(-39.1\ \text{kJ mol}^{-1}/RT),\quad 223 \le T \le 290\ \text{K},\ k^{HH}(298) = 17\,000\ \text{s}^{-1} \quad (23)$$

$$k^{HD} = 2k^{HD}_{AC\rightarrow DB} = 10^{11.4}\exp(-45.6\ \text{kJ mol}^{-1}/RT),\quad 267\ \text{K} \le T \le 306\ \text{K},\ 2k^{HD}_{AC\rightarrow DB}(298) \approx 2600\ \text{s}^{-1} \quad (24)$$

$$k^{DD} = 2k^{DD}_{AC\rightarrow DB} = 10^{11.9}\exp(-49.7\ \text{kJ mol}^{-1}/RT),\quad 298\ \text{K} \le T \le 323\ \text{K},\ 2k^{DD}_{AC\rightarrow DB}(298) \approx 1400\ \text{s}^{-1} \quad (25)$$

The kinetic isotope effects at 273 K are similar to those for the liquid state; i.e.

$$k^{HH}/k^{DD} \approx 17,\ k^{HD}/k^{DD} \approx 1.9 \quad (26)$$

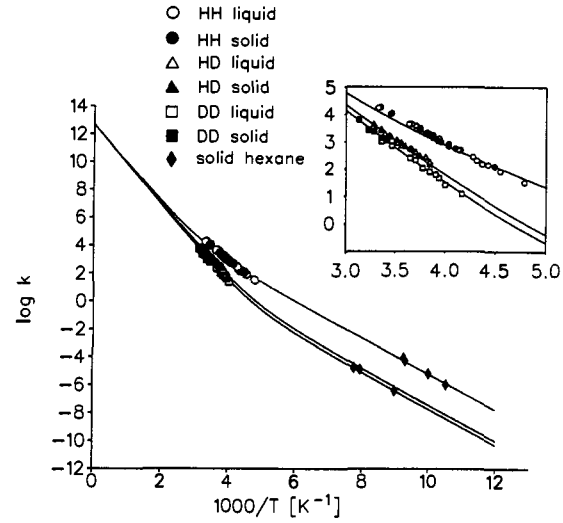

Figure 9. Arrhenius diagram of the tautomerism of porphyrin. The rate constants k correspond to the quantities $2k^{LL}_{AC\rightarrow DB}$, LL = HH, HD, and DD: (○) HH process; (△) HD process; (□) DD process in porphyrin dissolved in toluene-d_8; (●) HH process, solid; (▲) HD process; (■) DD process in solid porphyrin; (♦) HH and DD processes in solid hexane according to ref 30.

The Arrhenius diagram of the different isotopic reactions is shown in Figure 9, where filled-in symbols represent the solid state and open symbols represent the liquid solution in toluene-d_8. Figure 9 also includes data obtained for the thermal tautomerism of porphyrin embedded in solid hexane.[30] The solid curves were calculated using a modified Bell[47] tunneling model as discussed below.

Discussion

Kinetic HH/HD/DD Isotope Effects. The fact that the rate constants of the tautomerism of porphyrin-*HH*, porphyrin-*HD*, and porphyrin-*DD* (Figure 1) are the same both for toluene-d_8 as solvent and for the monoclinic phase, as illustrated in Figure 9, is remarkable. Moreover, in the solid state the degeneracy of the reaction is maintained within the margin of error. A similar phenomenon was observed for the case of *meso*-tetraphenylporphyrin (TPP) in the liquid and the tetragonal phase where only the HH reaction could be followed kinetically in the solid.[9] The rate constants of the tautomerism of the parent compound are significantly larger than those of TPP. At 298 K, the TPP tautomerism is approximately 3 times slower than in the parent. For both compounds, the kinetic HH/HD isotope effects are large and the kinetic HD/DD isotope effects are small. At 273 K, we find for porphyrin that $k^{HH}/k^{DD} \cong 17$, a value which is smaller than the value of 29 observed for TPP at the same temperature.[9] By contrast, the kinetic HD/DD isotope effects are much smaller and similar for both compounds; i.e., $k^{HD}/k^{DD} \cong 1.9$ for porphyrin and 2.0 for TPP[9] at 273 K. As shown recently,[8c,9,37-39] large kinetic HH/DD isotope effects and kinetic HD/DD isotope effects around 2 are typical for degenerate intramolecular double-proton-transfer reactions in relatively rigid molecular frames which involve two consecutive single-proton-transfer steps via an intermediate; i.e.

$$k^{HH}/k^{DD} = PS \cong P,\ k^{HD}/k^{DD} = 2/(P^{-1} + S^{-1}) \cong 2,\quad \text{for } P \gg 1,\ S \approx 1 \quad (27)$$

The three isotopic reaction rate constants depend only on the value of the primary kinetic H/D isotope effect P of the proton in flight; the bound mobile proton contributes a secondary kinetic H/D isotope effect S to the reaction. S is close to 1 when the

(47) Bell, R. P. *The Tunnel Effect in Chemistry*; Chapman and Hall: London, 1980.

secondary isotope effect is small. In the case of the oxalamidine tautomerism, this interpretation of isotope effects in terms of a stepwise proton motion could be further corroborated by finding strong kinetic solvent effects due to the formation of highly polar intermediates.[39] If the zero-point energies of the vibrations involving the bound proton decrease in the transition state, as in the case of intermolecular reactions where hydrogen bond compression is facile, S increases substantially.[37] As discussed in the Theoretical Section (see eq 11), eq 27 is also valid when the double-proton transfer is combined with 90° rotations, as long as $K = 1$. Equation 11 was visualized in Figure 3a.

If the degeneracy of the reaction is lifted, eq 27 is no longer valid. When the equilibrium constant of tautomerism K is much smaller than 1, a different set of isotope effects can be expected.[8c] In this case the relation

$$k^{HH}/k^{DD} = P,\ k^{HH}/k^{HD} = 2P/(P+1) \cong 2 \qquad (28)$$

holds in good approximation. Experimentally, this result has been verified recently for *meso*-tetraphenylchlorin, which represents a chemically perturbed porphyrin.[8c] As discussed in the Theoretical Section (see eq 11), eq 28 is also valid for the solid state when the proton transfer is nondegenerate and where the observed degeneracy is restored by fast 90° rotational jumps preceding or succeeding proton transfer according to Figure 2. In other words, when the degeneracy of the proton-transfer steps in solid porphyrin is lifted and the degeneracy is restored by 90° rotational jumps, the observed symmetric rate constants k^{HD} are expected to increase from the value $2k^{DD}$ to the value $k^{HH}/2$. Thus, the observation that $k^{HH}/k^{DD} \cong 17$ and $k^{HD}/k^{DD} \cong 2$ at 273 K for the tautomerism of porphyrin both in the liquid and in the solid state indicates that the degeneracy of the double-proton-transfer steps is maintained in the solid state.

Tautomerism, Rotational Jumps, and Structure of Monoclinic Porphyrin. As discussed in the Theoretical Section, rotational 90° jumps do not modulate the isotropic ^{15}N chemical shifts when the tautomerism is degenerate and are, therefore, difficult to detect by ^{15}N CPMAS NMR. Such jumps may, therefore, be present but would also be characterized by an equilibrium constant of 1 within the margin of error. The interesting finding of Frydman et al.[29] that the correlation times obtained from longitudinal rotating frame ^1H relaxation experiments are affected by deuteration in the inner proton sites and that they exhibit the same energy of activation as the tautomerism found by ^{15}N CPMAS NMR remains puzzling and requires further studies, for example, NMR experiments on porphyrin deuterated in the carbon sites or ^{13}C labeled in the *meso*-positions.

It is, therefore, obviously difficult to reconcile the ^{15}N NMR observation of proton disorder in polycrystalline porphyrin with the X-ray crystallographic structure of monoclinic porphyrin reported by Chen and Tulinsky (C&T)[15] in terms of the reaction network of Figure 2. Our NMR results are, therefore, in better agreement with the structure of Webb and Fleischer (W&F), who reported half-hydrogens on the four nitrogen atoms.[12] As mentioned in the introduction, the problem with the W&F structure was that some electron density was found in the porphyrin center, attributed to the presence of 5–10% Cu–porphyrin, although such an impurity could not be detected through any other method. C&T attributed the proton disorder observed in the W&F structure to the effects of the putative metalloimpurity assumed to form a solid solution with monoclinic porphyrin.[15] This idea was supported by the finding that pure *meso*-tetraphenylporphyrin (TPP) is triclinic with ordered protons but that a tetragonal solid solution with Ag–TPP is formed in which the protons are disordered.[21] These phenomena have indeed been verified by ^{15}N CPMAS NMR,[9,22] where it is found that triclinic TPP is subject to a nondegenerate proton tautomerism with equilibrium constants $K < 1$; by contrast, tetragonal cocrystals of the type $[Ni\text{–}TPP\text{-}^{14}N_4]_{0.1}[TPP\text{-}^{15}N_4]_{0.9}$ can be prepared where $K \approx 1$.[9,23] The X-ray powder diffraction patterns of pure triclinic TPP and of the cocrystals were dissimilar due to the differing crystal structures. By contrast, the W&F and C&T structures are very alike with the exception of the location of the inner protons. As shown in Figure 10a, the two structures exhibit the same monoclinic crystal symmetry, the same unit cell dimensions, and almost the same locations of the carbon atoms, nitrogen atoms, and hydrogen atoms in the carbon sites in the unit cell. The powder patterns calculated here for both structures did not differ significantly; they were compatible with the experimental pattern obtained for the material used in this NMR study. The concept of invoking a Cu impurity in order to explain the disorder in the W&F structure is therefore not without problems.

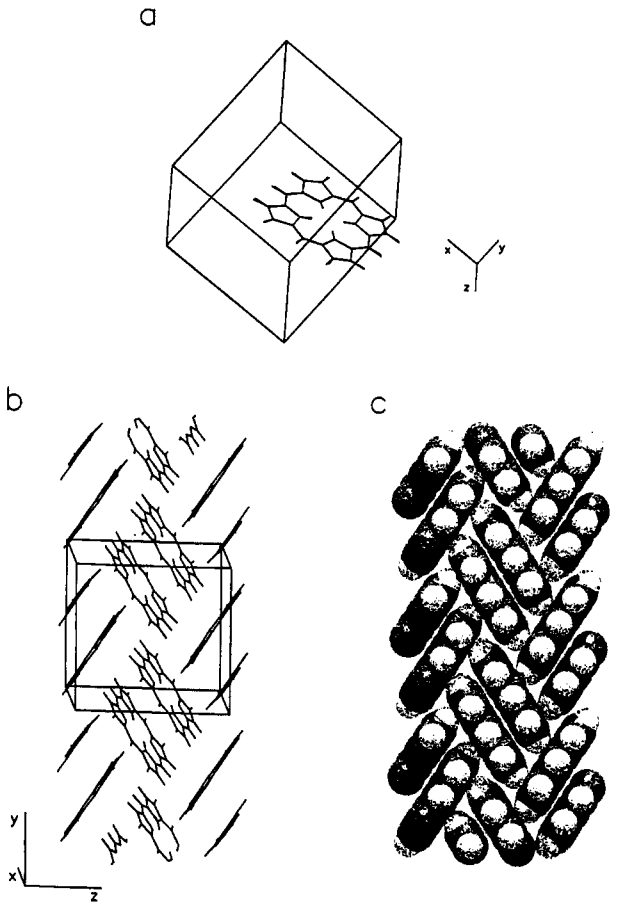

Figure 10. Packing diagrams for monoclinic porphyrin according to refs 12 and 14: (a) superposed W&F and C&T structures which agree within the margin of error except for the location of the inner protons; (b) ball and stick model including unit cell; (c) space filling model.

Regarding the discussion of the possibility of rotational 90° molecular jumps, it is interesting to take a look at the packing diagrams of porphin, based on the W&F or C&T structures[12,14] shown in Figures 10b and c. The molecules are very tightly packed. Note the stacking of porphyrins with perpendicular ring planes. Each porphyrin is located in a cell of the dimensions 10.2 Å × 10.2 Å × 3.42 Å. The porphyrin diagonal is 11.7 Å. Hypothetical 90° molecular jumps would, therefore, involve very large distortions either of the rotating molecule or of the cell space. Both processes obviously require large energies of activation, indicating that rotational jumps in porphyrin should be rather slow processes.

Interaction of Solid Porphyrin with Water. As stated in the previous sections, we observed that H_2O or D_2O penetrates solid porphyrin where a slow intermolecular proton exchange between the water protons and the mobile porphyrin protons takes place. We were thus able to deuterate and reprotonate polycrystalline porphyrin completely via the gas phase or by adding liquid water

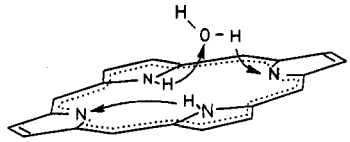

Figure 11. Model for the exchange of the inner protons of porphyrin with a water molecule in the solid state.

to the samples. Reproducible rate constants of the intramolecular HH, HD, and DD tautomerism were observed in all cases, independent of the manner in which deuteration or reprotonation was achieved. In preliminary experiments, we found that polycrystalline tetraarylporphyrins are also easily deuterated or reprotonated with gaseous or liquid water.

It is clear that the intermolecular proton exchange must take place in hydrogen-bonded complexes between water and porphyrin. One possibility is indicated in Figure 11, where the process is formulated as correlated inter- and intramolecular quadruple proton transfer. Other possible mechanisms could involve the formation of OH^- or H_3O^+ ions as intermediates. In addition, perhaps more than one water molecule could be required for the exchange to occur.

The main question which arises is how the water molecules and the porphyrin molecules come in contact with each other. Naturally, in the first step, water is adsorbed from the gas phase on the porphyrin crystal surfaces. A crude calculation based on the porphyrin crystal structure and an average size of the microcrystals used (1 mm × 1 mm × 0.2 mm) shows that the fraction of porphyrin molecules in surface layers should not exceed a value of 1–2%, meaning that if proton exchange between porphyrin and water only takes place on the surface, one should only expect a minimal degree of deuteration of porphyrin, in contrast to the experiment indicating a complete deuteration.

It is therefore tempting to assume that monoclinic porphyrin is capable of incorporating some water. In the case of tetraarylporphyrins, it is well-known that these molecules are "sponges" for various solvents[48] which are incorporated in large cavities and channels; recrystallizing TPP from *o*-xylene leads to an incorporation of the solvent in defined positions. In fact, the possibility of the formation of "aquoporphyrin" was considered by W&F,[12] but evidence for the water incorporation was poor. However, if the water positions are not well-defined and its mobility is high, this guest is not easily detected by X-ray crystallography. On the other hand, by NMR we were unable in this study to detect water in samples of porphyrin dissolved in organic solvents after exposure of the solid to water vapor, indicating that the actual quantity of water in solid porphyrin might be small.

The incorporation of larger water amounts also seems unlikely, as there seem to be no free cavities in the crystal, as illustrated in Figure 10. It is, however, conceivable that single water molecules or water clusters are, to a minor degree, incorporated in free lattice spaces, i.e. crystal defects. Water transport would then take place by defect diffusion involving both displacements of the water and the porphyrin molecules. It is conceivable that the two species are, in the defects, subject not only to translational but also to rotational diffusion. Finally, the possibility that the water remains on the surfaces but that diffusion at elevated temperatures enables each porphyrin molecule once reach the surface layer in which the deuteration process then takes place cannot completely be excluded but seems, nevertheless, unlikely.

In order to solve the problems raised, it will be necessary to look directly, via solid-state NMR, at suitably deuterated solid porphyrin in order to detect water and obtain information on its mobility as well as to perform tracer experiments from which diffusion constants of porphyrin in the solid state could be determined.

(48) Byrn, M. P.; Curtis, C. J.; Khan, A. I.; Sawin, P. A.; Tsurumi, R.; Strouse, C. E. *J. Am. Chem. Soc.* **1990**, *112*, 1865.

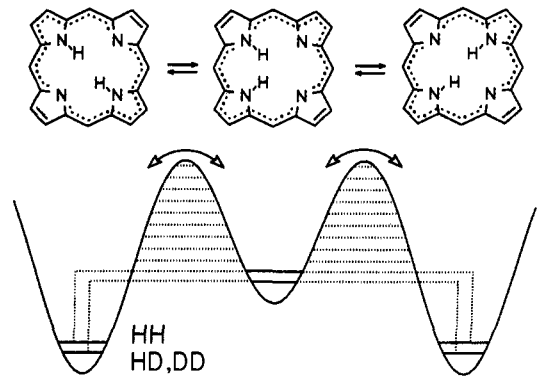

Figure 12. Tunneling model for the stepwise HH, HD, and DD transfer in porphyrin.

Complete Arrhenius Curve of the Tautomerism of Porphyrin. Apart from all the unsolved problems regarding the crystal structure of monoclinic porphyrin, it is clear that one can expect the outcome of the foregoing studies not to significantly affect the discussion of the mechanism of the proton tautomerism in this molecule. The observation made that the rate constants of all isotopic reactions are independent of the phase led us also to include in Figure 9 the rate constants obtained for the tautomerism of porphyrin in solid hexane using optical methods.[30] Although the degeneracy of both tautomers is lifted in this phase, the equilibrium constants of tautomerism were estimated to be close to unity,[30] indicating that the average $(k_{12} + k_{21})/2$ should be a good estimate of a hypothetical rate constant k in solid hexane for the case where $K = 1$. The validity of this assumption was recently verified for triclinic and tetragonal TPP.[23] Therefore, the construction of single Arrhenius curves of the HH, HD, and DD migration in porphyrin neglecting effects of the different environments is justified. The approximation[30] to compare the low-temperature kinetic data of the tautomerism of porphyrin with the high-temperature data of TPP in the liquid state[5,23] is then no longer necessary. This approximation is reasonable but not precise, as the rate constants of both compounds differ by a factor of 3 at room temperature. Nevertheless, the data in Figure 9 support the nonlinearity of the Arrhenius curves of the porphyrin tautomerism discussed previously.[30] The low-temperature deviations are less than those estimated many years ago in the case of TPP in liquid solution, where by NMR it was difficult to distinguish effects arising from slow molecular rotational diffusion and from the tautomerism.[5-7] These problems are overcome by the combination of the various kinetic methods used to construct Figure 9.

It is clear that, according to Bell,[47] nonlinear Arrhenius curves indicate a tunnel mechanism at low temperatures.[47] Evidence of a tunnel contribution even at room temperature can be inferred from the large primary kinetic isotope effects P, which are larger than those obtained recently for the stepwise tautomerism of azophenine[38] and of oxalamidine.[39] On the other hand, at low temperatures P does not increase as expected for a classical kinetic isotope effect.

The question then arises as to whether it is possible to reproduce the Arrhenius curves in Figure 9 in a quantitative way. The calculation of such curves should, in principle, be carried out on the basis of a realistic *ab initio* surface using a theory of chemical reaction rates which takes multidimensional tunneling of protons into account. On the other hand, a semiclassical reaction model of the type proposed recently for TPP/porphyrin by Zerbetto et al.[34] would be appropriate. Such calculations are, however, beyond the scope of this study. Instead, we consider a one-dimensional tunneling model of Bell[47] for the barrier region of the stepwise proton transfer, as presented previously[30] and as shown in Figure 12. In contrast to the Bell model, tunneling can only occur in the hatched regions, i.e. requires a minimum energy E_m. This

quantity is mainly determined by the energy of the intermediate but may also contain terms arising from the reorganization of the molecular skeleton before the proton transfer occurs. Secondary isotope effects are neglected; i.e., the HH and the DD reactions of porphyrin are treated as normal H or D transfers, and the rate constants of the HD reaction are generated using eq 27. According to the usual Bell treatment, an inverted parabola is used as an effective barrier. In contrast to the Bell model, we prefer to define different barrier heights E_d^L, L = H, D, and widths $2a^L$ for the isotopic reactions.[7,37b] Defining $\Delta\epsilon$ as the difference of the vibrational zero-point energies in the initial state and the transition state of the H and the D reaction, it follows that[7,37b]

$$E_d^D = E_d^H + \Delta\epsilon, \text{ and } 2a^D = 2a^H(E_d^D/E_d^H)^{1/2} \qquad (29)$$

The effective tunneling masses are $m^H = 1$ and $m^D = 2$. The calculation of the different Arrhenius curves using a computer program described previously[7,37b] is straightforward. The adaptable parameters are E_d^H, E_m, $2a^H$ and, in addition, the overbarrier frequency factor $A^H = \sqrt{2}(A^D)$.

In the computer program employed, the rate constants of all isotopic reactions could be fitted simultaneously. As shown in Figure 9, we obtained the best fit using the following parameters: E_m = 24.0 kJ mol^{-1}, E_d^H = 30.2 kJ mol^{-1}, $2a$ = 0.9 Å, $A = 10^{12.7}$ s^{-1}, and $\Delta\epsilon$ = 1.8 kJ mol^{-1}. The fit is not perfect, which is not surprising in view of the great number of approximations made.

It is interesting to calculate the classical primary kinetic isotope effect at 273 K according to the relation

$$P = \exp(-\Delta\epsilon/RT) \qquad (30)$$

The value of approximately 2 which we obtained is significantly smaller than the observed value of 17 and smaller than the effects calculated in terms of transition-state theory.[46,49,50] The frequency factor of $A^H \approx A_D \approx 10^{12.7}$ s^{-1} employed in the calculations of Figure 9 is a typical value for a unimolecular reaction, exhibiting a vanishing activation entropy. As mentioned above, when a term arising from the reorganization of the molecular skeleton is neglected, the minimum energy required for tunneling to occur determines the energy difference between the *cis*-tautomers and the *trans*-tautomers. E_m is obtained from the slope of the Arrhenius curves at low temperature and is similar for the HH and the DD reaction. Extrapolation of the low-temperature Arrhenius curves to $1/T = 0$ leads to an apparent low-temperature frequency factor on the order of 10^{-8} s^{-1} for the HH reaction. The inverse of this value is a crude estimate of the lifetime of the *cis*-intermediate before decay by tunneling. This value is very short and therefore, it is not surprising that the *cis*-intermediates have not yet been observed by optical hole-burning methods.

The remaining quantity left to be discussed concerns the value of the barrier width $2a$ = 0.9 Å. This value relates well to the geometry of porphyrin, for which one expects a proton-transfer distance of about 1.8 Å. Although the physical significance of these parameters should not be taken too seriously, they are in a range which is plausible.

Conclusions

The porphyrin tautomerism represents a unique case where rate constants of a double-proton transfer and the kinetic HH/HD/DD isotope effects are the same in liquid solution and in the bulk solids. The latter are consistent with a stepwise reaction pathway. An interesting interaction of solid porphyrin with water was observed: both gaseous or liquid D_2O or H_2O is able to completely deuterate or reprotonate polycrystalline porphyrin, probably via water incorporation in lattice defects and their diffusion. The absence of matrix effects on the rate constants of tautomerism allows the construction of the Arrhenius curves in a very wide temperature range, also taking into account the rate constants determined previously using optical methods for porphyrin dissolved in hexane. The Arrhenius curves are nonlinear, as expected for tunneling at low temperatures via the *cis*-intermediate. In approximation, the data can be interpreted within the framework of the Bell tunneling model, but their interpretation in terms of foregoing reaction models would be desirable. The kinetic isotope effects obtained for the solid state indicate that the degeneracy of the double-proton-transfer steps is maintained in the monoclinic polycrystalline porphyrin studied and is in agreement with the crystal structure reported by Webb and Fleischer.[12] Thus, we do not find evidence of proton tautomerism between nondegenerate tautomers followed by 90° jumps. Nevertheless, unsolved, interesting problems remain, especially regarding the interaction of porphyrin and of other organic solids with water.

Acknowledgment. We thank Mrs. I. Brüdgamand and Professor H. Harte, Institut für Anorganische und Analytische Chemie, Freie Universität Berlin, for characterizing the porphyrin by X-ray crystallography. In addition, we thank the Deutsche Forschungsgemeinschaft, Bonn-Bad Godesberg, the Stiftung Volkswagenwerk, Hannover, and the Fonds der Chemischen Industrie for financial support.

Appendix

In this section we describe in more detail the ^{15}N CPMAS NMR line-shape analysis of solid porphyrin on the basis of the reaction scheme illustrated in Figure 2. Because of the absence of scalar spin–spin coupling, the ^{15}N CPMAS NMR line-shape equation of a given ^{15}N atom in porphyrin can be easily set up using known rules.[45] If ρ'_i is the transverse density matrix element of the ^{15}N atom in state i, the following set of coupled equations is obtained

$$\frac{d\rho'_i}{dt} = -2\pi i\nu_i\rho'_i - \sum_{j\neq i} k_{ij}\rho'_i + \sum_{j\neq i} k_{ji}\rho'_j,\ i,j = 1,16 \qquad (A1)$$

ν_i is the chemical shift of the ^{15}N atom in state i. Setting $\nu_i = \nu_{NH}$ when the nitrogen is protonated and $\nu_i = \nu_N$ when it is nonprotonated, one can, by addition and taking eq 1 into account, show that eq A1 reduces to

$$\frac{d}{dt}\rho_1 = -i\nu_{AH}\rho_1 - (k_{1,2} + k_{1,4} + 2k_{1,5})\rho_1 + (k_{2,1} + k_{4,1})\rho_2 + 2k_{5,1}\rho_5$$

$$\frac{d}{dt}\rho_2 = -i\nu_A\rho_2 - (k_{2,1} + k_{4,1} + 2k_{5,1})\rho_2 + (k_{1,2} + k_{1,4})\rho_1 + 2k_{1,5}\rho_6$$

$$\frac{d}{dt}\rho_5 = -i\nu_{AH}\rho_5 - (k_{2,1} + k_{4,1} + 2k_{5,1})\rho_5 + (k_{1,2} + k_{1,4})\rho_6 + 2k_{1,5}\rho_1 \qquad (A2)$$

$$\frac{d}{dt}\rho_6 = -i\nu_A\rho_6 - (k_{1,2} + k_{1,4} + 2k_{1,5})\rho_6 + (k_{1,2} + k_{1,4})\rho_5 + 2k_{5,1}\rho_2$$

where

$$\rho_1 = \rho'_1 + \rho'_3 + \rho'_9 + \rho'_{11},\ \rho_2 = \rho'_2 + \rho'_4 + \rho'_{10} + \rho'_{12},\ \rho_5 = \rho'_5 + \rho'_7 + \rho'_{13} + \rho'_{15},\ \rho_6 = \rho'_6 + \rho'_8 + \rho'_{14} + \rho'_{16} \qquad (A3)$$

Equation A2 represents a similar equation one would set up for

(49) Melander, L.; Saunders, W. H. *Reaction Rates of Isotopic Molecules*; John Wiley & Sons: New York, and Toronto, 1980.
(50) Gandour, R. D.; Schowen, R. L. *Transition States of Biochemical Processes*; Plenum Press: New York, 1978.

the simplified reaction network of Figure 2a but with a differing definition of rate constants.

The numerical calculation of the NMR line shape starting from equations of the type of eq A2 has been described and need not be repeated here.[45] Therefore, we discuss in the following only some limiting cases of eq A2.

A. *Symmetrical Case with $K = 1$.* States 1 and 5 as well as states 2 and 6 become indistinguishable, and eq A2 reduces to the symmetric two-state problem

$$\frac{d}{dt}\rho_{NH} = -(2\pi i\nu_{NH} + k)\rho_{NH} + k\rho_N, \frac{d}{dt}\rho_N = -(2\pi i\nu_N + k)\rho_N + k\rho_{NH} \quad (A4)$$

where

$$k = k_{1,2} + k_{1,4} = k_{2,1} + k_{4,1}, \rho_{NH} = \rho_1 + \rho_5 \text{ and } \rho_N = \rho_2 + \rho_6 \quad (A5)$$

Note that the line shape does not depend on the rate constant $k_{1,5}$ of rotation.

B. *Unsymmetrical Case with $K \ll 1$.* The states of higher energy are nonobservable, metastable intermediates. Using the usual steady-state assumption of formal kinetics (i.e., that the time dependence of the concentrations of the intermediate eliminates a symmetric two-state problem similar to eq A4) results in the observed rate constant of proton transfer being given by

$$k = \frac{(k_{1,2} + k_{1,4})2k_{5,1}}{k_{2,1} + k_{4,1} + 2k_{5,1}} + \frac{2k_{1,5}(k_{1,2} + k_{1,4})}{k_{2,1} + k_{4,1} + 2k_{5,1}} = 2\frac{(k_{1,2} + k_{1,4})2k_{5,1}}{k_{2,1} + k_{4,1} + 2k_{5,1}} = 2\frac{2k_{1,5}(k_{1,2} + k_{1,4})}{k_{2,1} + k_{4,1} + 2k_{5,1}} \quad (A6)$$

where eq 3 has been taken into account. In the case where the rotation is faster than the proton transfer, it follows that

$$k = 2(k_{1,2} + k_{1,4}) \text{ for } k_{5,1} \gg k_{2,1}, k_{4,1} \quad (A7)$$

In the case where the rotation is slower than the proton transfer, we obtain from eq 9

$$k = 4k_{1,5} \text{ for } k_{5,1} \ll k_{1,2}, k_{1,4} \quad (A8)$$